MICROWAVE-TO-TERAHERTZ PROPERTIES AND APPLICATIONS OF GRAPHENE

Norbert Klein[1], Stephen Hanham[1], Mohammad Adabi[1], Olena Shaforost[1], Ling Hao[2]

[1] Imperial College London, Department of Materials, South Kensington Campus, London, SW7 2AZ, United Kingdom
[2] National Physical Laboratory, Hampton Rd, Teddington TW11 0LW, United Kingdom

The unique electronic properties of graphene are attractive for a variety of device applications in microwave-to-terahertz technology. For frequencies up to several 100 GHz, graphene behaves like a dispersion-free resistive sheet, the value of its sheet resistance can be controlled by an external gate voltage. This property enables the realization of electrically controllable attenuators, fast switches and modulators for frequencies up to the terahertz range. Due to hot electrons in graphene, highly sensitive and ultrafast graphene THz detectors have been demonstrated, which have a strong potential to outperform other detector types operated at room temperature. In the terahertz-to-midinfrared range, the excitation of plasmon type surface waves enables promising application as label free electromagnetic biosensor devices.

INTRODUCTION

Graphene is one of the great promises for future micro- and nano-electronic applications. At microwave-to-terahertz frequencies, a graphene layer behaves like a resistive sheet which exhibits almost no dispersion up to 1 THz. The value of the sheet resistance can be controlled by an external gate voltage, which enables the realization of fully integrated devices like voltage controlled attenuators and fast modulators for frequencies up to the terahertz range [1]. Moreover, fast and highly sensitive THz detector for room temperature operation have been realized based on hot electron effects in graphene [2,3]. This contribution focusses on the microwave-to-terahertz properties of graphene, and perspectives for system applications are discussed briefly.

WAFER-SCALE GRAPHENE

Among the methods being developed for the deposition of large area graphene, chemical vapour deposition on copper and subsequent transfer on a target substrate has turned out to be the most efficient and flexible method yielding large area and single layer graphene coatings of high quality [4]. Fig. 1 shows the combined PVD-CVD system within the Department of Materials at Imperial College London for 4'' in-situ graphene deposition on copper thin films, the insert shows an optical microscopy image and a Raman spectrum indicating smooth and low defect graphene with a high degree of single layer growth. The flexibility of the transfer process enables graphene deposition on a wide range of substrate materials including high resistive silicon (HRS), quartz and plastics as materials for mm wave and THz integrated devices.

Graphene layers can be patterned to any shape by standard lithographic processes using oxygen plasma as a selective etching method [5].

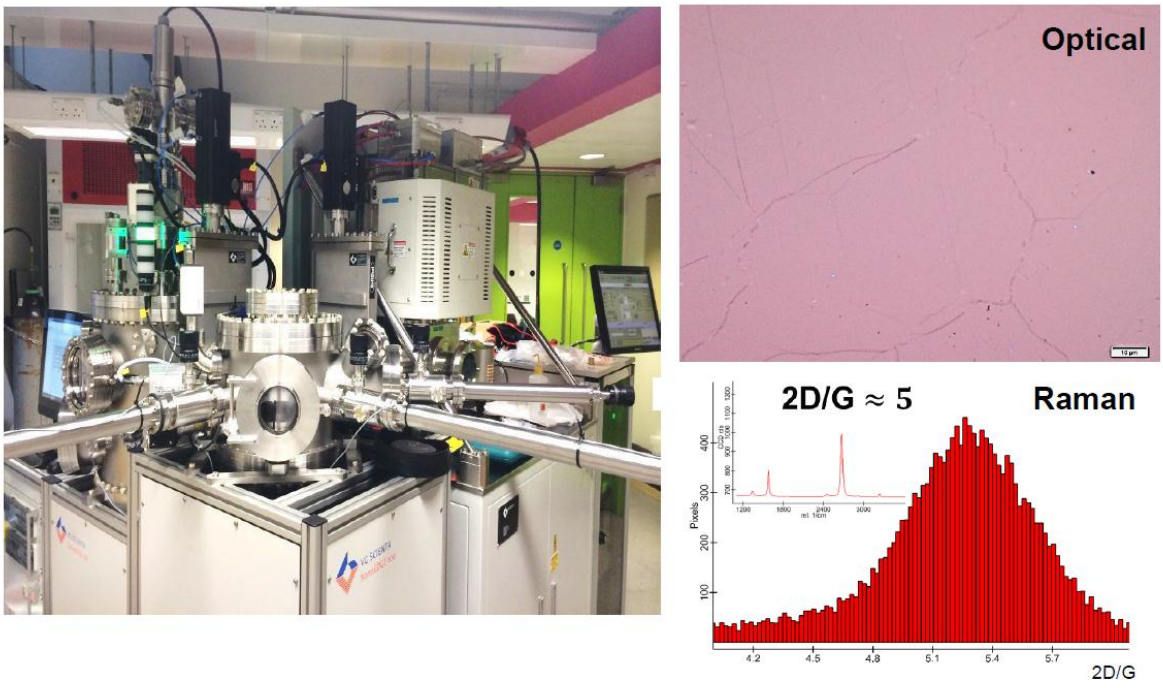

Fig 1. Combined graphene CVD / metal PVD system for 4" wafer scalable graphene deposition and microscopy and Raman results indicating high-quality single layer graphene.

MICROWAVE AND THZ CHARACTERIZATION OF GRAPHENE

As one of the most flexible and accurate methods for surface impedance measurements of graphene at microwave frequencies, we have employed a ceramic high-Q cylindrical dielectric resonator (DR) exited in the $TE_{01\delta}$ mode [6]. The DR is arranged inside a metal shielding cavity which hosts coaxial coupling loops, the adjustable distance between the DR and the aperture in the top lid of the shielding cavity defines the strength of cavity loading by inductive coupling to the graphene layer being placed on top of the aperture (see Fig. 2). Graphene substrates need to be semi-transparent for microwaves, their loss contribution to the total quality factor of the resonant cavity mode can be determined by calibration measurements with empty substrates. In case of HRS covered with a thin dielectric layer (native or thermal SiO_2, thin dielectric layers deposited on top of HRS) as substrate a gate voltage can be applied across the gate dielectric between HRS and graphene by employing electrical contacts outside the cavity aperture [1].

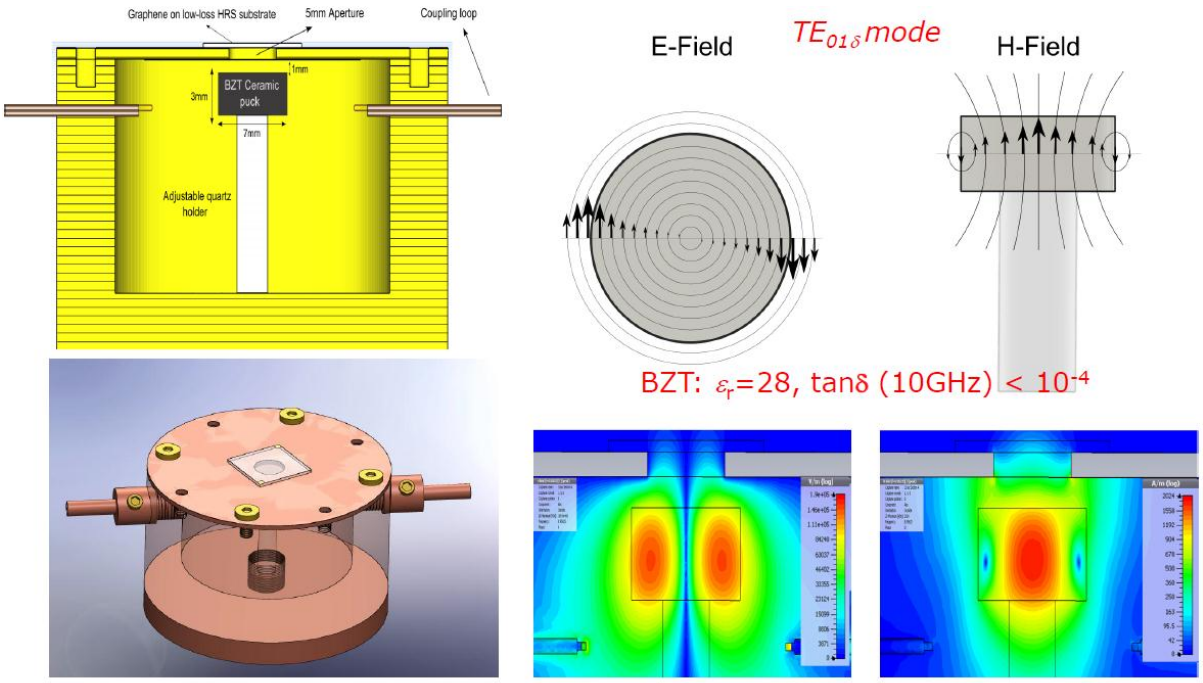

Fig. 2: Experimental setup for microwave characterization of large area graphene layers and FET structures by a dielectric loaded cavity.

Due to the ideal resistive sheet properties, the presence of graphene results in a reduction of the Q factor but almost no change of resonance frequency. Fig. 3 shows the variation of the resonance curve due to changes of the gate voltage between graphene and the HRS substrate (right). The variation of S_{21} over the bandwidth of the cavity illustrates the basic functionality of an electronic attenuator, however, the 2dB dynamic does not reflect any optimized design. Employing calibration methods described in [1,6] the sheet resistance as a function of gate voltage can be extracted from the measured Q factors (left). The results show good agreement with DC measurements on the same sample. The maximum of the sheet resistance at positive gate voltages represents charge neutrality of graphene (Dirac point). Due to defect charges at the gate oxide-graphene interface the Dirac point often is at positive bias voltage, sample/device annealing can change it towards zero voltage.

Typically, the ratio between R_{max} and R_{min} is 4 - 5, but it does not represent a fundamental limit and is therefore subject to improved graphene – gate insulator – interface quality, which strongly depends on the processing conditions. Since the cavity Q factor is proportional to the sheet resistance (if other cavity losses are neglected), a factor of 5 (on-off ratio) corresponds to a maximum tuning range of the cavity insertion loss at resonance by $10 \cdot \log_{10}(5^2) \approx 14$ dB.

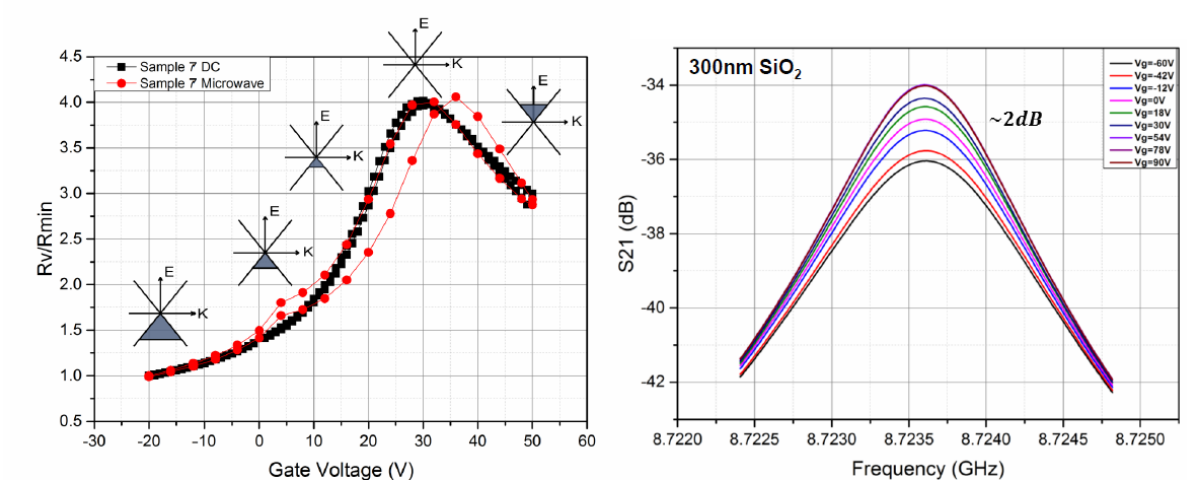

Fig. 3: resonance transmission curve for the cavity shown in Fig. 2 for a graphene FET structure with 300 nm thick SiO_2 gate dielectric for different values of the gate voltage (right), extracted sheet resistance as function of gate voltage (left).

Fig. 4 shows the time response of S_{21} at resonance to pulsed gate voltage variations for different values of the bias voltage offset. The time constant varies between several 10 and several 100 milliseconds, with a maximum around the Dirac point where the RC time constant of the large area capacitor is at maximum due to a maximum of graphene's sheet resistance and the effect of graphene's quantum capacitance on the total gate capacitance [1,7]. Since graphene's intrinsic carrier response is on the picosecond timescale, the dynamic behaviour scaled down to micron sized devices is expected to be in the sub-nanosecond range. As being analysed in [1], the maximum of time constant around the Dirac point can be explained by the maximum of the sheet resistance and a maximum of the total capacitance due to the influence of the carrier density dependent quantum capacitance of graphene [7].

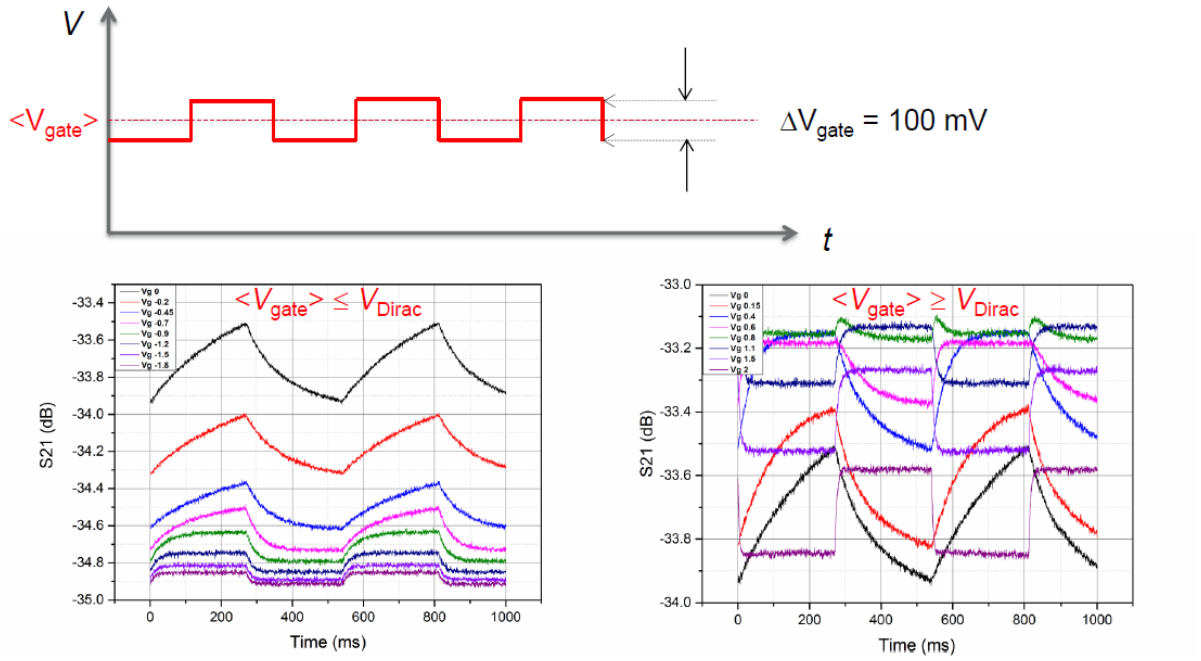

Fig. 4: Dynamic response of the cavity transmission at resonance for different gate voltages below (p-doped) and above (n-doped) the Dirac point.

The setup shown in Fig. 5 allows quasioptical reflectance / transmission measurements of large area graphene layers which enables an accurate study of the weak frequency dependence of the sheet resistance in the frequency range of 100-500 GHz. Moreover, a wire grid polarizer is aligned at 45 degree with respect to the polarization of the Gaussian beam (which is generated by horn launchers and parabolic mirrors from the waveguide output ports of the mm wave VNA transceiver heads). If the graphene sample is arrange inside a strong magnetic field, the cross polarized component can be analysed to determine the carrier density by means of the AC Hall effect. Hence, our system represents a most comprehensive tool to qualify graphene layers for device application at mm wave frequencies.

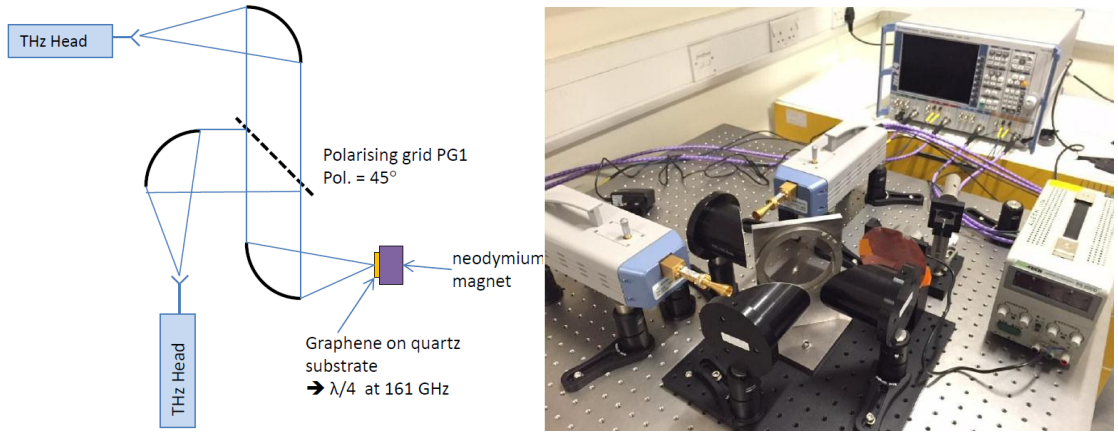

Fig. 5: Experimental setup to measure the mm wave reflection in the presence of a high magnetic field. The analysis of the cross polarized component enables the investigation of the AC Hall effect without electrical contacts (from S. Hanham, Imperial College London, to be published).

PERSPECTIVES FOR APPLICATIONS IN WIRELESS COMMUNICATION AND SENSING SYSTEMS

As an example for an integrated device, Fig. 6 shows the design and results of simulations for a coplanar switch based on variable resistors made from gate-biased graphene layers. In combination with fast graphene THz detectors [3,4], low cost point-to multipoint wireless communication links with tenths of Gbit/s speed at (sub) mm wave carrier frequencies will be enabled, but sources based on multiplied solid state devices still prevent a fully integrated and low cost solution. For near-field imaging applications in security and bio-medicine the possible use of thermal THz sources would benefit from fast and low cost THz detectors and modulators by enabling ultrafast and sensitive lock-in detection. Although these applications address niches at the current state, the broader commercial utilization is often hampered by the high system costs of THz sources and waveguide components.

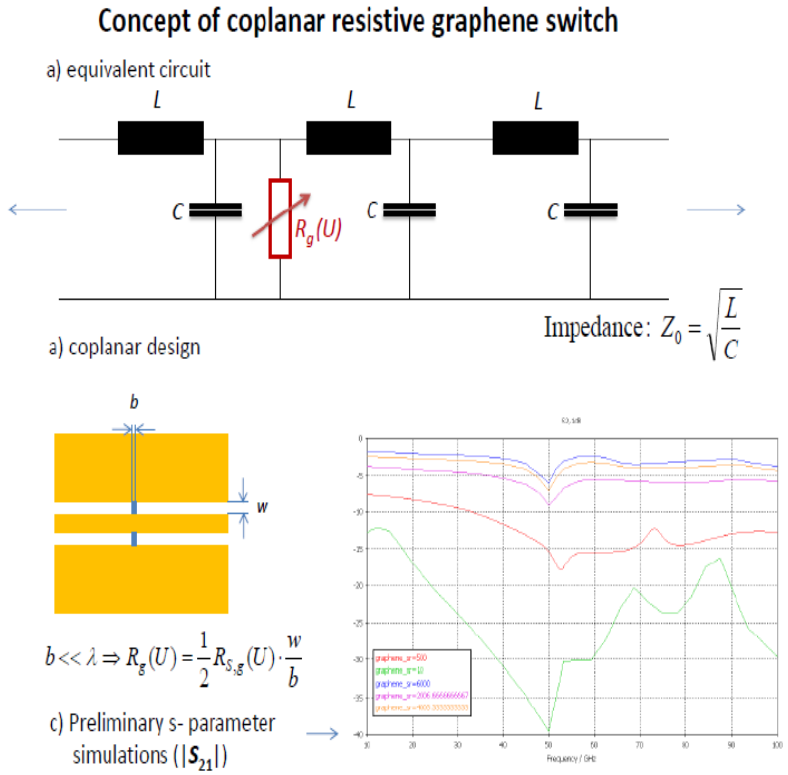

Fig. 6: Design and simulation of a coplanar switch based on gate voltage controlled graphene resistors.

CONCLUSION

Graphene has a strong potential to bring the THz frequency range to a broader use and enable the development of new applications. The reproducible manufacturing and processing of wafer scale graphene and the development of microwave-to-terahertz characterization and

qualification methods and developments of standards are important steps towards a broader commercial utilization.

REFERENCES

[1] M. Adabi and N.Klein et al. (Imperial College London), detailed publication in progress

[2] Xinghan Cai et al., Nature Nanotechnology **9**, 814 (2014)

[3] D. Spirito et al., Appl. Phys. Lett. **104**, 061111 (2014)

[4] Yi Zhang et *al.,* Chem. Res. **46,** 2329 (2013)

[5] Ji Feng et al., Nanoscale **4**, 4883 (2012)

[6] O. Shaforost et al., J. Applied Phys. **117**, 0021-8979 (2015)

[7] E. Yu et al., Phys. Rev. B **91**, 075416 (2015)